Density functional theory calculations for ethylene carbonate-based binary electrolyte mixtures in lithium ion batteries

Mahesh Datt Bhatt[1] and Colm O'Dwyer[1,2]

[1] *Department of Chemistry, University College Cork, Cork, Ireland*

[2] *Tyndall National Institute, Lee Maltings, Cork, Ireland*

Abstract

The density functional theory (DFT) calculations have been performed to investigate the interaction of Li^+ with various organic solvents widely used as Li ion rechargeable battery electrolytes such as ethylene carbonate (EC), propylene carbonate (PC), dimethyl carbonate (DMC), diethyl carbonate (DEC), ethyl methyl carbonate (EMC); and their EC-based binary mixtures at the level of B3LYP/6-31G (d). The interaction of Li^+ with these solvents has been calculated in terms of electronic structures of clusters of the mixtures of organic solvents including a lithium ion. The main objective of our investigation is to help in understanding a stable and enhancing ionic transfer at graphite/electrolyte interface assisted by the mixtures of the solvents. The calculated results favor the stability of EC-based binary mixtures and high EC-content binary mixture systems. In infrared (IR) vibrational spectra, the IR active modes of the solvent show significant changes due to the cation-solvent interaction.

Key Words: Lithium ion battery, electrolytes, solvent, SEI layer, electronic structure

E-mail of corresponding author: mbhatt54@yahoo.com

1. Introduction

Lithium ion batteries with liquid electrolytes are becoming popular power sources for portable electronic devices and electric vehicles [1, 2]. A lithium ion battery is made up of a graphite carbon anode, a non-aqueous organic electrolyte that acts as an ionic path between two electrodes and a transition-metal oxide (such as $LiCoO_2$, $LiMn_2O_4$ and $LiNiO_2$) cathode. The most common electrolytes are mixtures of alkyl carbonates such as ethylene carbonate (EC), propylene carbonate (PC), linear carbonates such as dimethyl carbonate (DMC), diethyl carbonate (DEC), ethyl methyl carbonate (EMC), and lithium salts such as $LiClO_4$, $LiPF_6$, $LiBF_4$ and $LiAsF_6$. It is well known that cyclic life and stability of Li-ion batteries are dependent on the formation of an organic/inorganic layer at the graphite anode/electrolyte interface, usually known as the solid electrolyte interphase (SEI) film [3-6]. Thus, it is clear that the physical properties of SEI film and the interactions between SEI film and the graphite anode also play an important role determining the formation and the quality of the SEI film.

The SEI film formation differs significantly among the various organic solvents. For example, an SEI film is formed in an ethylene carbonate (EC) based electrolyte, while exfoliation of graphite occurs and no SEI is formed in the propylene carbonate (PC) based electrolytes [7-11]. However, PC is used as a practical battery electrolyte solvent with vinylene carbonate (VC) as an additive, since an SEI layer is formed in the presence of VC [12]. It is generally believed that VC facilitates SEI film formation on a graphite anode surface. However, the mechanism of such SEI film formation due to addition of VC in PC-based electrolytes is not clear yet and is, thus, the subject of intensive research [13-20]. In overall, we can say that SEI formation depends on several factors such as the reactivity of solvent, the physical properties of the film, and the interaction of the film with the graphite anode surface, given the same Li salt. Yang et al. [21] reported that only EC gets decomposed in a battery solvent of EC/DEC or EC/DMC binary mixtures to contribute to the SEI formation, and that DMC and DEC mainly

improve viscosity and conductivity. Although the reductive decomposition of EC has been extensively investigated by theoretical studies [22, 23], little has been reported on the reduction of DMC, DEC and EMC.

Whether the environment is liquid, or polymeric, or solid, understanding the nature of the lithium ion coordination is crucial to understanding the conductivity mechanism. For Lithium ion batteries and liquid electrolytes, cyclic and linear organic solvents, and their mixtures have been proven to be efficient, especially with respect to cyclability. A mixture of two or more solvents allows the design of different electrolyte properties in a wider range and thus to enhance the performance. The application of ab-initio calculations to liquid electrolytes for lithium batteries was pioneered by Blint and his calculations on different ether and carbonyl oxygen containing species and their mixtures and the coordination of lithium ions [24, 25]. Blint extrapolated that a four-coordinated complex would be dominant, which was also supported by Gibb's free energy calculations in Klassen et al. and Wang et al. Blint has also considered di-methyl ether, di-ethyl ether, acetone and water [24], and acetaldehyde [25], some recent studies have used acetonitrile [26] and γ-butyrolactone [27] as solvents. The later solvent has gained interest due to its wide liquid-phase temperature range (-42 to 206°C). In such context, we foresee the area of applying the first principle calculations to problems of battery electrolytes to prosper, as there are many outstanding issues with respect to the electrolyte decomposition in general and the formation and stability of the SEI layer in particular.

In this article, the density functional theory (DFT) is used to investigate the solvation of lithium ions in EC-based binary mixtures of non-aqueous electrolytes and to explain it at the molecular level. The optimized structures of organic solvents are shown in Fig. 1.

2. Computational Details

All clusters of organic electrolytes and their binary mixtures including a lithium ion are optimized by using B3LYP/6-31G (d) spin non-polarized calculations by means of

Restricted Hartree-Fock (RHF) mode. Restricted Hartree-Fock theory uses a single molecular orbital twice, once multiplied by α spin function and once multiplied by β spin function in the slater determinant. An isolated Li^+ is simulated in Gaussian by setting the charge +1 for a Li atom. In case of simulation of Li^+-S complex, it is assumed that: $(Li\text{-}S)^+ = Li^+ + S$. The density functional theory (DFT) calculations are performed with hybrid parameter B3LYP as implemented in Gaussian 09 [29]. The hybrid parameter B3LYP5 consists of exchange correlation function generalized gradient approximation (GGA) in the Becke [30], Lee-Yang-Parr [31], and VWN formula 5 [32]. The basis set is chosen as 6-31G (d) for our calculations. The approximate basis set superposition error (BSSE) [33] for all clusters is calculated using Counter Poise (CP) method and was observed to be negligibly small. The optimized structures of some mixtures are shown in Fig. 2. To confirm each optimized and stationary points and make zero point energy (ZPE) corrections, frequency analyses are done with the same basis set. Enthalpy and Gibb's free energy are obtained at 298.15 K. The charge distribution is analyzed by Mulliken population analysis.

3. Results and Discussions

The interaction of Li^+ with EC-based binary mixtures can be calculated in terms of the distance between Li^+ and carbonyl oxygen ($r_{Li^+\text{-}O}$), charges on Li^+ (q_{Li^+}), charges on carbonyl oxygen (q_O), and dipole moment (D) with the direction as illustrated in Table I. The primary results in Table I favor the stability of EC/DMC/Li^+ system (based on structural properties) and stability of EC/DEC/Li^+ system (based on dipole moment) as compared to other EC-based binary mixtures. In Table I, the Li^+-O bond distance is stable and seemingly invariant at higher EC concentrations, compared to all other systems and it is also indicated by change in the wavenumber shift in the IR vibrational response that could be due to this interatomic distance stability in the clusters. In general, with regard to the electrochemical stability especially with respect to the ability to form desirable SEI films in terms of the protective nature and ionic

resistance, EC/DMC/Li^+ or EC/DEC/Li^+ system is more stable than other EC-based binary mixtures [34].

The interaction strength between Li^+ and solvent mixtures can also be quantified by calculating the binding energy of the formation of the $[Li^+(EC)_x(S)]$ complexes (S = PC, DMC, DEC, EMC and their mixtures) as:

$\Delta E = E\,[Li^+(EC)_x(S)] - E\,[Li^+] - x * E\,[EC] - E\,[S]$

where $E\,[Li^+(EC)_x(S)]$, $E\,[Li^+]$, E [EC] and E [S] represent the total energy of $Li^+(EC)_x(S)$ complexes, Li^+, EC molecule, and co-solvent and their mixtures respectively. Similarly, Gibb's free energy (ΔG) and heat of formation (ΔH) for solvent mixtures can be calculated by using the relations: $\Delta G = G\,[Li^+(EC)_x(S)] - G\,[Li^+(EC)_{x-1}(S)] - G$ [EC]

and, $\Delta H = H\,[Li^+(EC)_x(S)] - H\,[Li^+(EC)_{x-1}(S)] - H$ [EC]

The coordination reaction that corresponds to free energy and heat of formation reactions can be written as $Li^+ + (EC)_{x-1} = Li^+(EC)_x$

The binding energy (ΔE), Gibb's free energy (ΔG), and heat of formation (ΔH) of $Li^+(EC)_x(S)$ complexes is listed in Table II. It should be noted from Table II that the binding energy, Gibb's free energy, and heat of formation are in the order EC/PC > EC/DEC > EC/EMC > EC/DMC for low EC-based binary mixtures and in the order EC/DMC > EC/DEC > EC/EMC > EC/PC for high EC-based binary mixtures. Our calculated results are fairly in agreement with the experimental results [35, 36]. The SEI composition greatly depends on the types of solvents. It seems that only EC is decomposed in a binary solvent mixture to contribute to the SEI formation, and that co-solvent of EC mainly improves viscosity and conductivity [21].

The optimized structure of EC as shown in Fig. 1 (a) is a five member ring containing two oxygen atoms with a carbonyl group located at the apex. The symmetry of EC is assumed to be C_{2v} with the ring being planar. EC has 24 fundamental modes of vibration. According to group theory, the number of vibrations of each irreducible representation is

$$\Gamma = 8a_1+4a_2+5b_1+7b_2$$

All the modes of vibrations are Raman-active while only a_1, b_1, and b_2 are infra-red active. The calculated infrared (IR) frequencies of particular modes of vibrations of isolated EC molecule and Li^+-EC complex at the level of B3LYP/6-31G (d) are listed in Table III [37]. To ease the comparison with the vibrational frequencies of the single EC molecule, the notation ν_i is used for the 24 modes of EC and ω_i is used for three modes where lithium is involved. Regarding the effect of the ion on the solvent molecules vibrational frequencies and considering the results for the structure of the solvated complexes, it seems reasonable to expect that the strongest effects will be found for [Li^+-EC] complex. It may be noticed that many of the frequencies of the single EC molecule coordinated to Li^+ are affected, for example, C=O frequency decreases from and C-O frequency increases from 1150.26 to 1271.05 cm^{-1}. Similar changes are found in particular IR modes of vibration regarding CH2 twisting, ring stretching and ring C=O bending due to cation-solvent interaction. The corresponding compared IR spectra for isolated EC molecule and Li^+-EC complex are shown in Fig. 3.

The interaction between Li^+ and solvent mixtures can be further computed by analyzing their infrared (IR) spectra in the 0-2000 cm^{-1} spectral range. The calculated IR frequencies at particular modes for EC-based binary mixtures are listed in Table IV. The compared IR spectra of EC-based binary mixtures are shown in Fig. 4(a)–(d). The spectra are presented so that the bands affected by the addition of Li^+ and coordination number of EC in the binary mixtures. The C=O frequency gradually increases and C-O frequency gradually decreases with increase in content of EC. Similar change can be seen in other IR modes of vibration. Such a change in the active IR modes of the solvent shows the stability of EC-based binary mixture and high EC-content binary mixtures due to the cation-solvent interaction. This result is fairly in agreement with the reference results [35, 38]. The Li^+-O distance is specifically invariant for the EC/DMC mixtures at EC concentrations greater than the initial concentrations, so solvent interactions that are mentioned in the conclusions could play a role in the vibrational energies of the carbonyl and C-O bonds. It is known that solvents with high dielectric permittivity formed

strongly structured electrolytes [39]. For example, the permittivity of EC is 89.8, while that of DMC is 3.1, so it can be said that the highly structured EC solvent is broken up by the low permittivity DMC component. It is the reason why EC/DMC binary solvent has higher ionic conductivity than EC/DEC and EC/EMC binary solvents [40]. In fact, the stability of EC/DMC solvent and high EC-content binary mixture is attributed to the high ionic conductivity of Li^+. In this way, such investigations favor the stability of EC-based binary mixtures in applications of lithium-ion batteries.

4. Conclusions

The density functional theory (DFT) calculations have been performed to investigate the interaction of Li^+ with various organic solvents widely used as Li ion rechargeable battery electrolytes such as ethylene carbonate (EC), propylene carbonate (PC), dimethyl carbonate (DMC), diethyl carbonate (DEC), ethyl methyl carbonate (EMC); and their EC-based binary mixtures at the level of B3LYP/6-31G (d). The interaction of Li^+ with these solvents has been calculated in terms of electronic structures of clusters of the mixtures of organic solvents including a lithium ion. The main objective of our investigation is to help in understanding a stable and enhancing ionic transfer at graphite/electrolyte interface assisted by the mixtures of the solvents. The calculated results favor the stability of EC-based binary mixtures and high EC-content binary mixture systems. In infrared (IR) vibrational spectra, the IR active modes of the solvent show significant changes due to the cation-solvent interaction.

Acknowledgements

This research has received funding from the Seventh Framework Programme FP7/2007-2013 (Project STABLE) under grant agreement n°314508.

References

[1] Armand M, Tarascon JM (2008) Nature 451:652-657

[2] Xu K (2004) Chem Rev 104:4303-4417

[3] Peled E (1979) J Electrochem Soc 126:2047-2051

[4] Peled E, Golodnitsky D, Ardel G (1997) J Electrochem Soc 144:L 208-L210

[5] Nazri G, Muller RH (1985) J Electrochem Soc 132:2050-2054

[6] Aurbach D, Daroux ML, Faguy PW, Yeager E (1987) J Electrochem Soc 134:1611-1620

[7] Eichinger G (1976) J Electrochem Soc 74:183-193

[8] Matsuura Y, Wang S, Mondori J (1995) J Electrochem Soc 142:2914-2918

[9] Winter M, Besenhard JO, Spahr ME, Novak P (1998) Adv Mater 10:725-763

[10] Jeong SK, Inaba M, Mogi R, Iriyama Y, Abe T, Ogumi Z (2001) Langmuir 17:8281-8286

[11] Peled E, Golodnitsky D, Pencier J, In Handbook of Battery Materials; Besenhard JO (1999) Ed; Wiley-VCH: New York, p 419-456

[12] Yoshio M, Nakamura H, Yoshitake H, Tanaka S (1997) U S Patent 5:669-681

[13] Shu ZX, McMillan RS, Murray JJ, Davidson IJ (1995) J Electrochem Soc 142:L161-L162

[14] Shu ZX, McMillan RS, Murray JJ, Davidson IJ (1996) J Electrochem Soc 143:2230-2235

[15] Ein-Eli Y, Thomas SR, Koch VR (1997) J Electrochem Soc 142:1159-1165

[16] Wrodnigg GH, Besenhard JO, Winter M (1999) J Electrochem Soc 146:470-472

[17] Foster DL, Behl WK, Wolfenstine J (2000) J Power Resources 85:299-301

[18] Moller KC, Santner HJ, Kern W, Yamaguchi S, Besenhard JO, Winter M (2003) J Power Sources 119:561-566

[19] Vetter J, Novak P (2003) J Power Sources 119:338-342

[20] Yoshitake H, Abe K, Kitakura T, Gong JB, Lee YS, Nakamura H, Yoshio M (2003) Chem Lett 32:134-135

[21] Yang CR, Wang YY, Wan CC (1998) J Power Sources 72 :66-70

[22] Wang YX, Nakamura S, Ue M, Balbuena PB (2001) J Am Chem Soc 123:11708-11718

[23] Han YK, Lee SU (2004) Theor Chem Acta 112:106-111

[24] Blint RJ (1995) J Electrochem Soc 142:696-702

[25] Blint RJ (1997) J Electrochem Soc 144:787-791

[26] Xuan X, Zhang H, Wang J, Wang H (2004) J Phys Chem A 108:7513-7515

[27] Masia M, Rey R (2004)J Phys Chem B 108:17992-18002

[28] Smart MC, Ratnakumar BV, Whitcanack LD, Chin KB, Surampudi S, Croft H, Tice D, Staniewicz R (2003) J Power Sources 119-121:349-358

[29] Frisch MJ, Trucks GW, Schlegel HB, Scuseria GE, Robb MA, Cheeseman JR, Scalmani G, Barone V, Mennucci B, Petersson GA, Nakatsuji H, Caricato M, Li X, Hratchian HP, Izmaylov AF, Bloino J, Zheng G, Sonnenberg JL, Hada M, Ehara M, Toyota K, Fukuda R, Hasegawa J, Ishida M, Nakajima T, Honda Y, Kitao O, Nakai H, Vreven T, Montgomery JA, Peralta JE, Ogliaro F, Bearpark M, Heyd JJ, Brothers E, Kudin KN, Staroverov VN, Kobayashi R, Normand J, Raghavachari K, Rendell A, Burant JC, Iyengar SS, Tomasi S, Cossi M, Rega N, Millam JM, Klene M, Knox JE, Cross JB, Bakken V, Adamo C, Jaramillo J, Gomperts R, Stratmann RE, Yazyev O, Austin AJ, Cammi R, Pomelli C, Ochterski JW, Martin RL, Morokuma K, Zakrzewski VG, Voth GA, Salvador P, Dannenberg JJ, Dapprich S, Daniels AD, Farkas O, Foresman JB, Ortiz JV, Cioslowski J, Fox DJ, Gaussian, Inc, Wallingford CT (2009) Gaussian 09, Revision A.1

[30] Pogrebnaya TP, Becke AD (1988) Phys Rev A 38:3098-3100

[31] Lee C, Yang W, Parr RG (1988) Phys Rev B 37:785-789

[32] Vosko SH, Wilk L, Nusair M (1980) Canad J Phys 58:1200-1211

[33] Boys SF, Bernardi F (1970) Mol Phys 19:553-566

[34] Smart MC, Ratnakumar BV, Surampudi S, (1999) J. Electrochem. Soc. 146:486-492

[35] Klassen B, Aroca R, Nazri M, Nazri GA (1998) J Phys Chem B 102:4795-4801

[36] Aroca R, Nazri M, Nazri GA, Camargo AJ, Trsic M, (2000), J. Sol. Chemistry 29: 1047-1060

[37] Bhatt MD, Cho MH, Cho KJ (2012) Modelling Simul Mater. Sci. Eng. 20:065004-065008

[38] Masia M, Probst M, Rey R (2004) J Phys Chem B 108:2016-2027

[39] Fawcett WR, Kloss AA, (1996) J. Chem. Soc. Faraday Trans. 92: 3333-3340

[40] Hayashi K, Nemoto Y, Tobishima S., Yamaki J (1999) Electrochim. Acta 44:2337-2344

Table I. Li^+-O distance, natural charges on Li^+, natural charges on carbonyl oxygen atom (EC, S = PC, DMC, DEC, EMC) and dipole moment of the mixtures

Complexes/ Mixtures	Distance between Li^+ and O (EC, S), $r_{Li^+\text{-}O}$(Å)	Charges on Li^+ (|e|)	Charges on O (EC, S) (|e|)	Dipole moment D (Debye)
EC/PC/Li^+ Ratio:				
1:1:1	1.8026, 1.7992	0.628	-0.539, -0.548	1.95
2:1:1	1.8754, 1.8699	0.495	-0.517, -0.526	2.56
3:1:1	1.9511, 1.9391	0.022	-0.972, -0.992	0.93
EC/DMC/Li^+ Ratio:				
1:1:1	1.7958, 1.7895	0.606	-0.540, -0.551	4.59
2:1:1	1.8762, 1.8454	0.989	-1.022, -0.958	4.09
3:1:1	1.9534, 1.9129	0.379	-0.500, -0.503	5.72
EC/DEC/Li^+ Ratio:				
1:1:1	1.7998, 1.7830	0.967	-1.100, -1.017	6.90
2:1:1	1.8848, 1.8436	0.466	-0.520, -0.533	5.83
3:1:1	1.8818, 1.8452	0.452	-0.512, -0.529	5.66
EC/EMC/Li^+ Ratio:				
1:1:1	1.7972, 1.7864	0.603	-0.538, -0.554	5.92
2:1:1	1.8843, 1.8477	0.474	-0.521, -0.531	6.37
3:1:1	1.9630, 1.9022	0.373	-0.501, -0.504	5.89

Table II. Binding energies ΔE (in kcal/mol), Gibbs free energies ΔG (in kcal/mol) and heats of formation ΔH (in kcal/mol) of mixtures at the level B3LYP/6-31G (d) at a temperature 298.15 K (1 hartree = 27.2 eV, 1 eV = 22.96 kcal/mol)

Isolated components/Reactions	ΔE	ΔG	ΔH
$Li^+ + EC \longrightarrow Li^+(EC)_1$	49.80	-47.42	-53.34
$Li^+ + PC \longrightarrow Li^+(PC)$	49.45	-47.18	-53.06
$Li^+ + DMC \longrightarrow Li^+(DMC)$	46.35	-33.48	-26.66
$Li^+ + DEC \longrightarrow Li^+(DEC)$	47.52	-34.07	-27.77
$Li^+ + EMC \longrightarrow Li^+(EMC)$	47.97	-33.88	-27.12
$Li^+(EC)_1 + PC \longrightarrow Li^+(EC)_1PC$	48.20	-33.87	-41.89
$Li^+(EC)_1PC + EC \longrightarrow Li^+(EC)_2PC$	26.51	-15.87	-25.03
$Li^+(EC)_2PC + EC \longrightarrow Li^+(EC)_3PC$	17.04	-7.16	-16.36
$Li^+(EC)_1 + DMC \longrightarrow Li^+(EC)_1DMC$	42.73	-29.01	-36.58
$Li^+(EC)_1DMC + EC \longrightarrow Li^+(EC)_2DMC$	28.18	-16.28	-26.06
$Li^+(EC)_2DMC + EC \longrightarrow Li^+(EC)_3DMC$	18.87	-7.16	-18.12
$Li^+(EC)_1 + DEC \longrightarrow Li^+(EC)_1DEC$	44.80	-30.44	-38.78
$Li^+(EC)_1DEC + EC \longrightarrow Li^+(EC)_2DEC$	27.03	-15.94	-25.38
$Li^+(EC)_2DEC + EC \longrightarrow Li^+(EC)_3DEC$	17.91	-5.83	-11.36
$Li^+(EC)_1 + EMC \longrightarrow Li^+(EC)_1EMC$	43.79	-30.41	-37.08
$Li^+(EC)_1EMC + EC \longrightarrow Li^+(EC)_2EMC$	26.78	-15.91	-25.12
$Li^+(EC)_2EMC + EC \longrightarrow Li^+(EC)_3EMC$	17.23	-4.26	-10.69

Table III. Calculated IR frequencies (cm^{-1}) at particular modes of vibrations for EC and Li^+-EC complex in the gas phase

EC		[Li^+-EC]			
Modes	v	Modes	v	Assignment	Shift
ν_3 (a)	1934.79	ν_3 (a)	1814.00	C=O stretching	-120.79
ν_6 (a)	1421.94	ν_6 (a)	1547.33	o. p. CH_2 twisting	125.39
ν_8 (a)	1150.26	ν_8 (a)	1271.05	O-C sym, C-C stretch	120.79
		ω_1(a)	531.66	ring Li^+-O stretching	
ν_{18} (b)	1245.55	ν_{17}(b)	1482.13	ring stretching	236.58
ν_{24} (b)	134.16	ν_{24} (b)	174.71	ring C=O bending	40.55
		ω_2 (b)	114.10	ring Li^+-O bending	
		ω_3 (b)	89.02	Li^+-O=C bending	

Table IV. Calculated Infrared (IR) frequencies (cm^{-1}) at particular modes of vibration for isolated EC molecule, Li^+-EC complex, and EC-based binary mixtures

Molecule/	IR frequencies at particular IR modes							
Mixtures	ν_3 (a)	ν_6 (a)	ν_8 (a)	ν_{18} (a)	ν_{24} (b)	ω_1 (a)	ω_2 (b)	ω_3 (b)
EC/PC/Li^+ Ratio:								
1:1:1	1823.30	1550.90	1259.45	1469.90	179.81	619.37	132.16	103.17
2:1:1	1837.59	1549.90	1230.86	1450.84	194.10	552.26	126.45	107.94
3:1:1	1861.42	1546.14	1211.80	1441.31	208.40	437.91	121.22	117.86
EC/DMC/Li^+ Ratio:								
1:1:1	1733.75	1547.33	1421.94	1472.10	174.71	662.48	139.18	58.93
2:1:1	1834.06	1537.30	1401.46	1462.06	194.77	576.80	119.12	53.91
3:1:1	1854.12	1532.28	1391.43	1447.02	214.83	410.86	104.07	53.91
EC/DEC/Li^+ Ratio:								
1:1:1	1834.06	1552.31	1366.35	1507.21	169.27	667.50	134.16	68.96
2:1:1	1837.28	1547.35	1361.33	1482.13	199.79	576.80	114.10	48.90
3:1:1	1839.08	1542.33	1356.32	1477.11	204.80	486.52	94.04	38.87
EC/EMC/Li^+ Ratio:								
1:1:1	1829.04	1552.35	1381.40	1442.00	174.71	662.48	134.16	58.93
2:1:1	1834.06	1522.25	1376.38	1467.08	204.80	566.77	124.13	53.91
3:1:1	1854.12	1507.21	1366.35	1447.02	214.83	456.00	109.09	43.88

Figure Captions

Fig. 1 Optimized structure of Ethylene Carbonate (EC), Propylene Carbonate (PC), Dimethyl Carbonate (DMC), Diethyl Carbonate (DEC), and Ethyl Methyl Carbonate (EMC)

Fig. 2 Optimized structures of $Li^+(EC)_x(S)$ (S = PC, DMC, DEC, and EMC; x = 1-3) complexes

Fig. 3 Compared IR spectra of isolated EC molecule and Li^+-EC complex

Fig. 4 Compared IR spectra of (a) $EC_x/PC/Li^+$; (b) $EC_x/DMC/Li^+$; (c) $EC_x/DEC/Li^+$; and (d) $EC_x/EMC/Li^+$ complexes (x = 1-3)

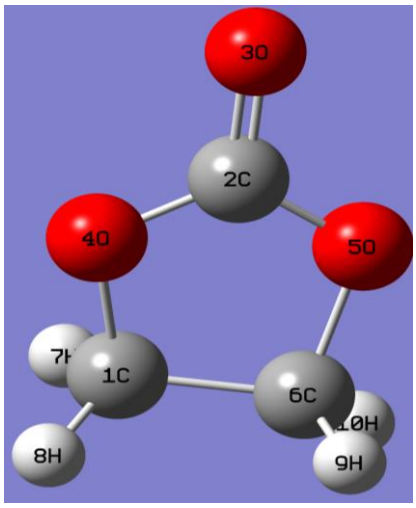
3O
2C
4O
5O
7H
1C
6C
10H
8H
9H

(a)

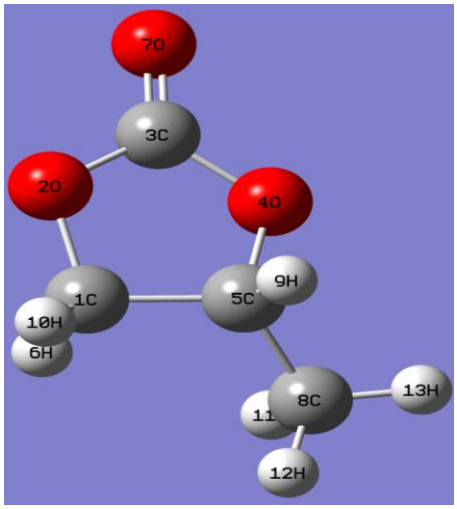
7O
3C
2O
4O
9H
1C
5C
10H
6H
8C
13H
12H

(b)

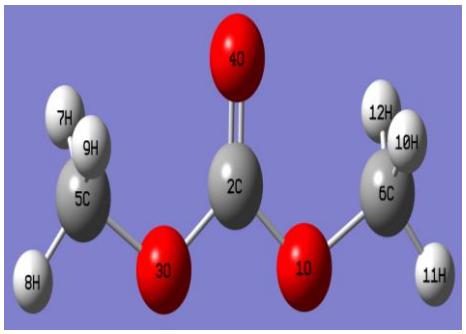
4O
7H
9H
12H
10H
2C
5C
6C
8H
3O
1O
11H

(c)

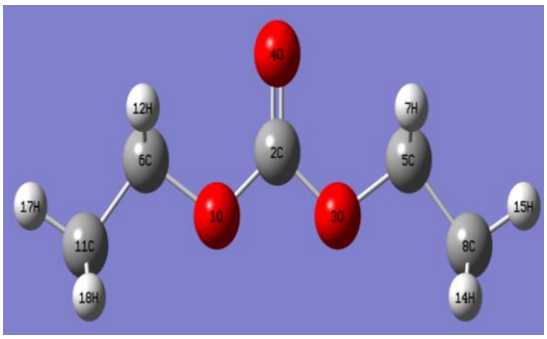
4O
12H
7H
6C
2C
5C
17H
1O
3O
15H
11C
8C
18H
14H

(d)

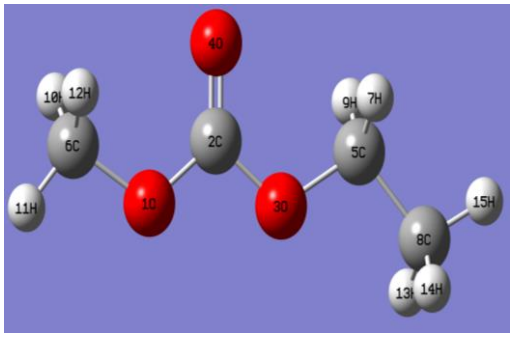
4O
12H
9H
7H
6C
2C
5C
11H
1O
3O
15H
8C
14H

(e)

Fig. 1

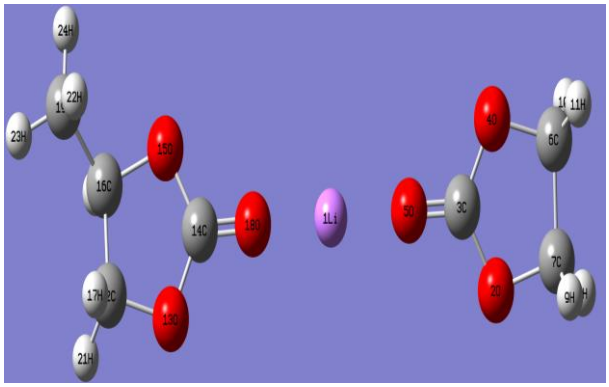

(a)

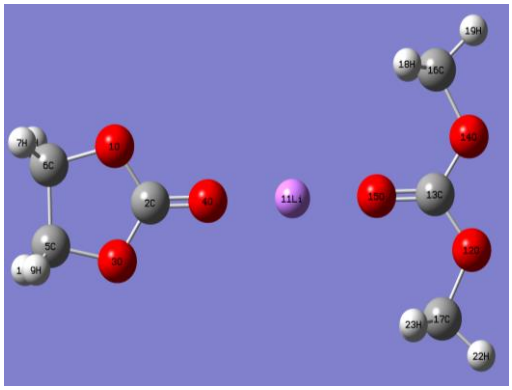

(b)

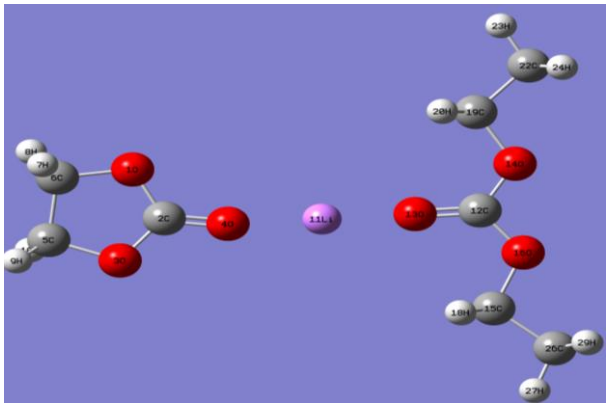

(c)

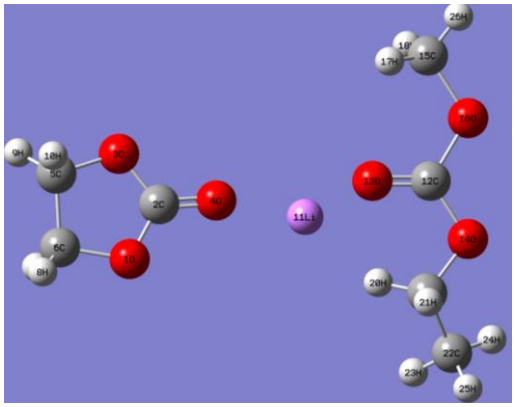

(d)

Fig. 2

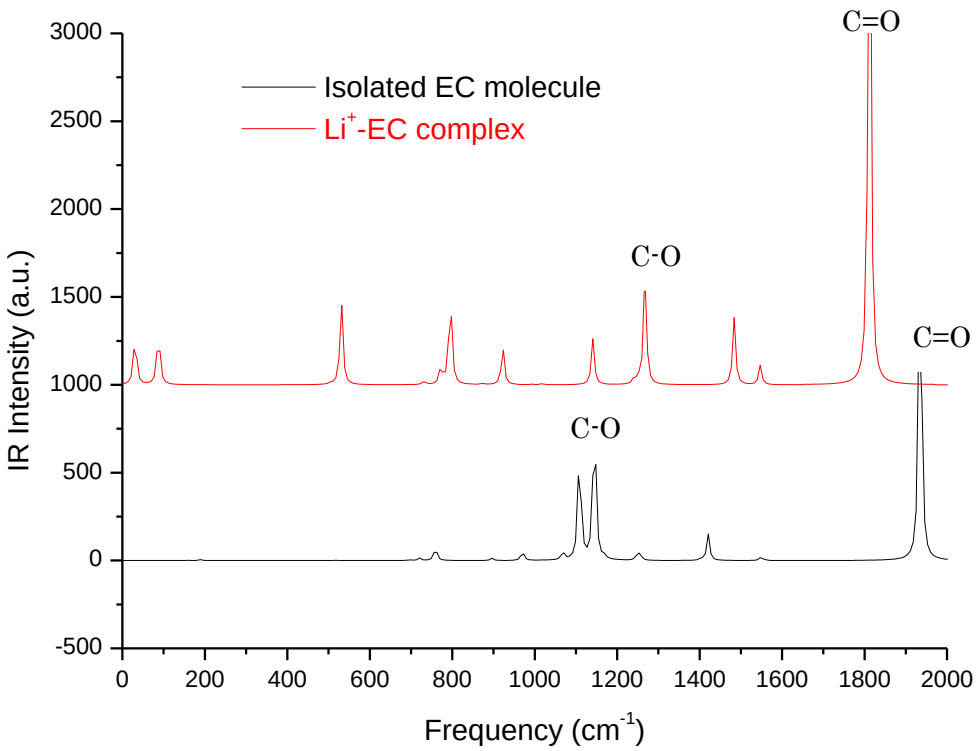
C=O
Isolated EC molecule
Li+-EC complex
C-O
C=O
C-O
IR Intensity (a.u.)
3000
2500
2000
1500
1000
500
0
-500
0
200
400
600
800
1000
1200
1400
1600
1800
2000
Frequency (cm-1)

Fig. 3

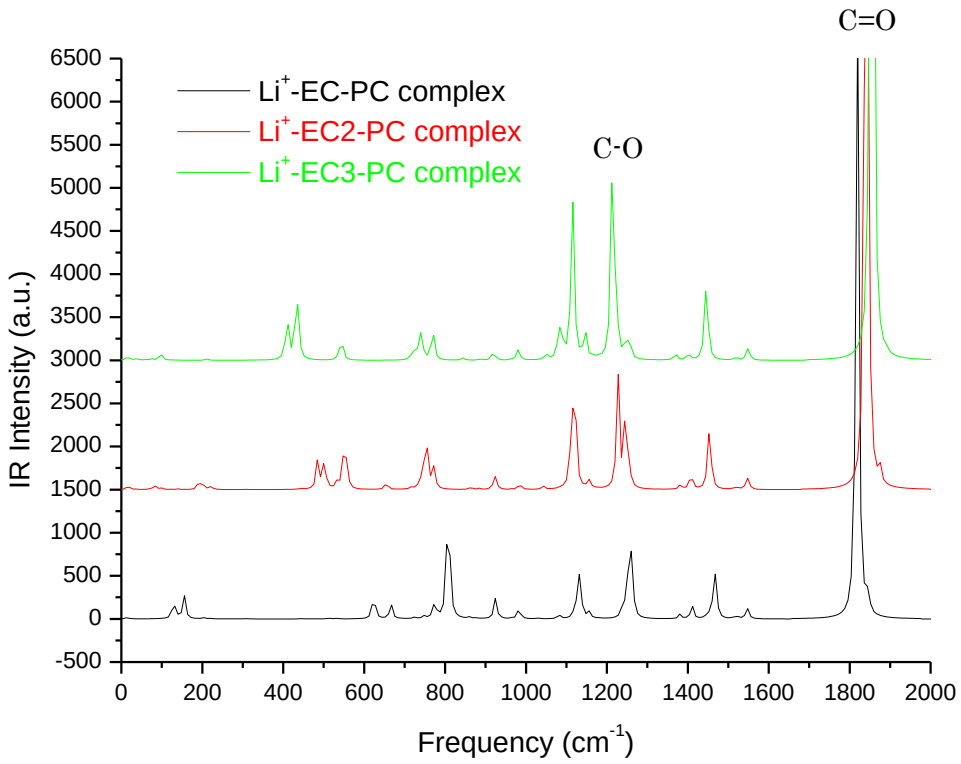
C=O
C-O
Li+-EC-PC complex
Li+-EC2-PC complex
Li+-EC3-PC complex
IR Intensity (a.u.)
Frequency (cm-1)

(a)

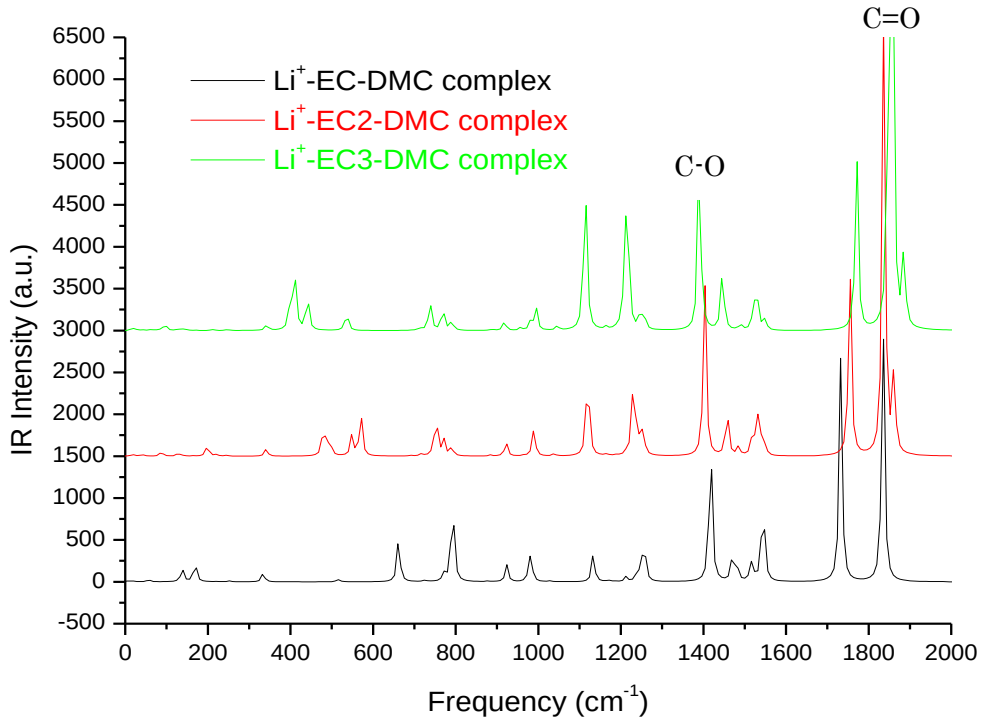
C=O
C-O
Li+-EC-DMC complex
Li+-EC2-DMC complex
Li+-EC3-DMC complex
IR Intensity (a.u.)
Frequency (cm-1)

(b)

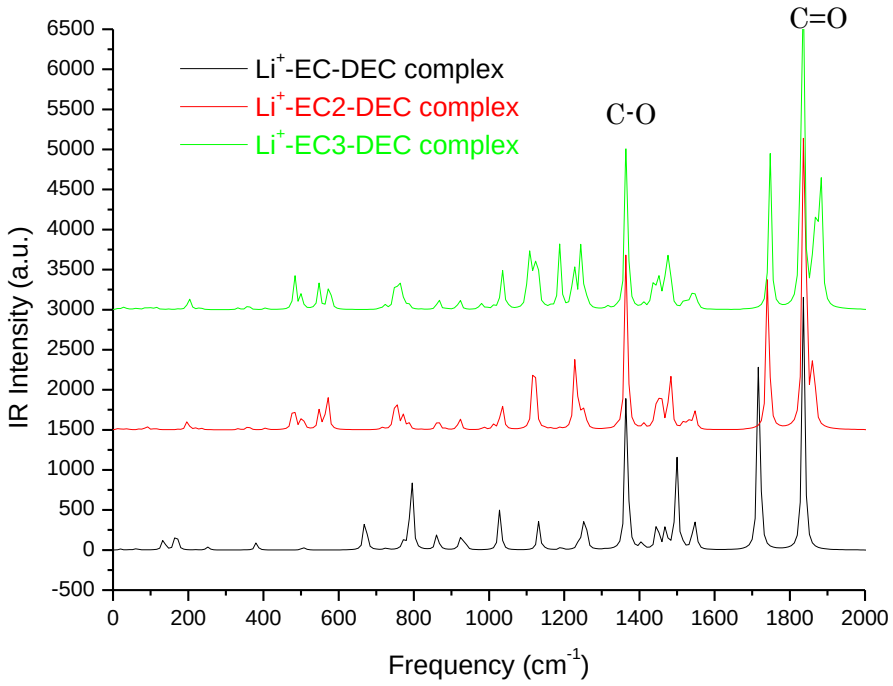
C=O
C-O
Li+-EC-DEC complex
Li+-EC2-DEC complex
Li+-EC3-DEC complex
IR Intensity (a.u.)
Frequency (cm-1)

(c)

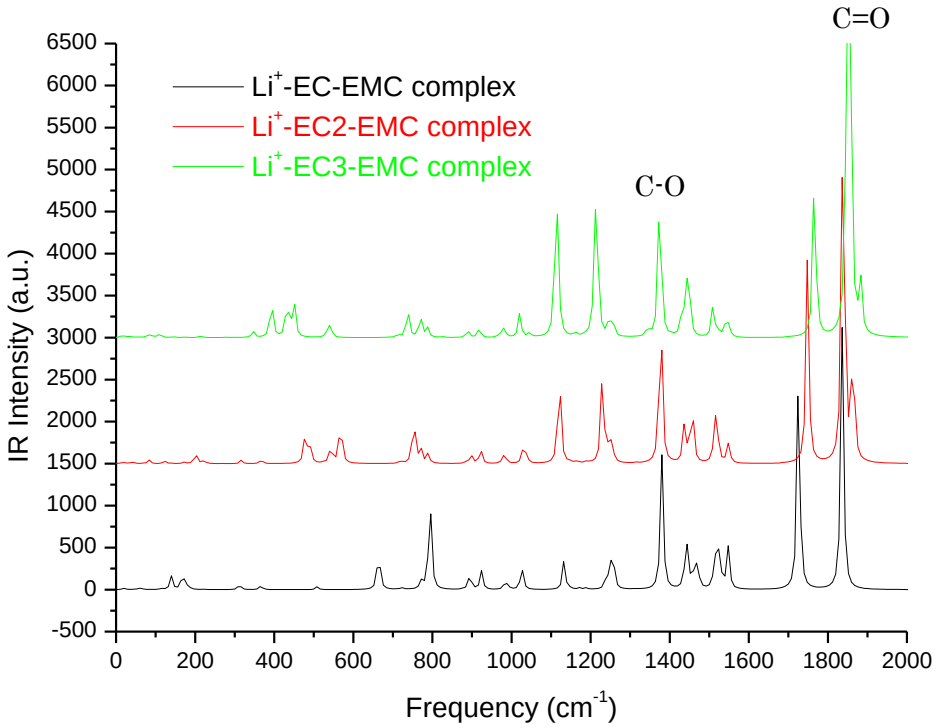
C=O
C-O
Li+-EC-EMC complex
Li+-EC2-EMC complex
Li+-EC3-EMC complex
IR Intensity (a.u.)
Frequency (cm-1)

(d)

Fig. 4